

## Supplemental materials for manuscript:

### Assessing formic and acetic acid emissions and chemistry in western U.S. wildfire smoke: implications for atmospheric modeling

Wade Permar<sup>1</sup>, Catherine Wielgasz<sup>1</sup>, Lixu Jin<sup>1</sup>, Xin Chen<sup>2</sup>, Matthew M. Coggon<sup>3</sup>, Lauren A. Garofalo<sup>4</sup>, Georgios I. Gkatzelis<sup>5</sup>, Damien Ketcherside<sup>1</sup>, Dylan B. Millet<sup>2</sup>, Brett B. Palm<sup>6</sup>, Qiaoyun Peng<sup>7</sup>, Michael A. Robinson<sup>3</sup>, Joel A. Thornton<sup>7</sup>, Patrick Veres<sup>3</sup>, Carsten Warneke<sup>3</sup>, Robert J. Yokelson<sup>1</sup>, Emily V. Fischer<sup>8</sup>, Lu Hu<sup>1</sup>

<sup>1</sup>Department of Chemistry and Biochemistry, University of Montana, Missoula, MT, USA.

<sup>2</sup>Department of Soil, Water, and Climate, University of Minnesota, St. Paul, MN, USA.

<sup>3</sup>Chemical Sciences Laboratory, National Oceanic and Atmospheric Administration, Boulder, CO, USA.

<sup>4</sup>Department of Chemistry, Colorado State University, Fort Collins, CO, USA.

<sup>5</sup>Institute of Energy and Climate Research, IEK-8: Troposphere, Forschungszentrum Jülich GmbH, Jülich, Germany.

<sup>6</sup>Atmospheric Chemistry Observations & Modeling Laboratory, National Center for Atmospheric Research, Boulder, CO, USA.

<sup>7</sup>Department of Atmospheric Sciences, University of Washington, Seattle, WA, USA.

<sup>8</sup>Department of Atmospheric Science, Colorado State University, Fort Collins, CO, USA.

Correspondence: Wade Permar ([wade.permar@umontana.edu](mailto:wade.permar@umontana.edu))

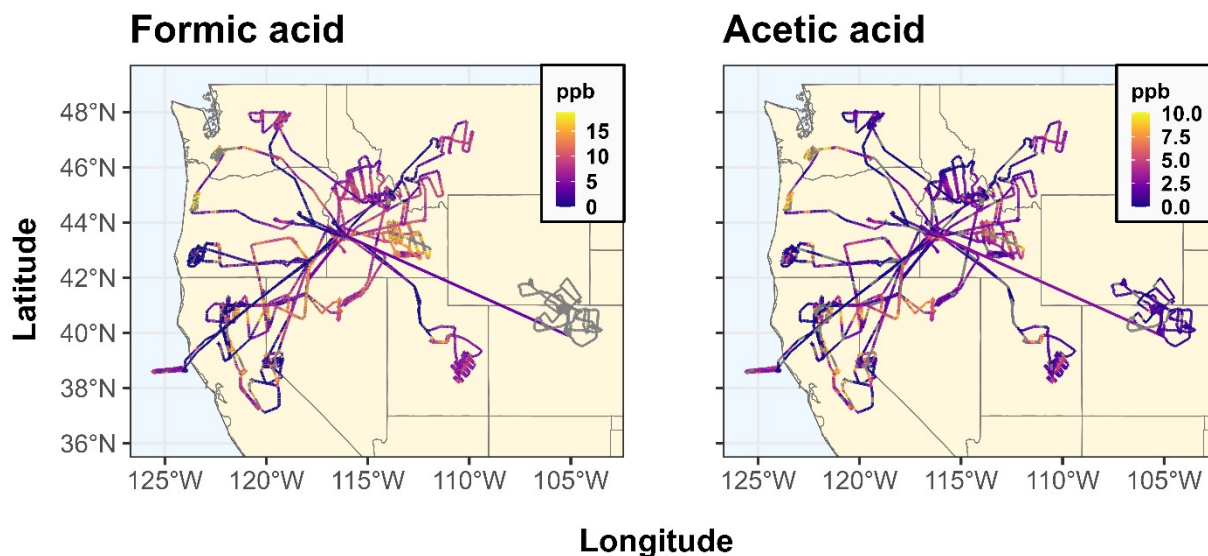


**Figure S1.** Flight tracks for WE-CAN research flights colored by formic acid (I-CIMS) and acetic acid (PTR-ToF) mixing ratios (ppb). Maximum concentrations are limited to the 95th percentile.

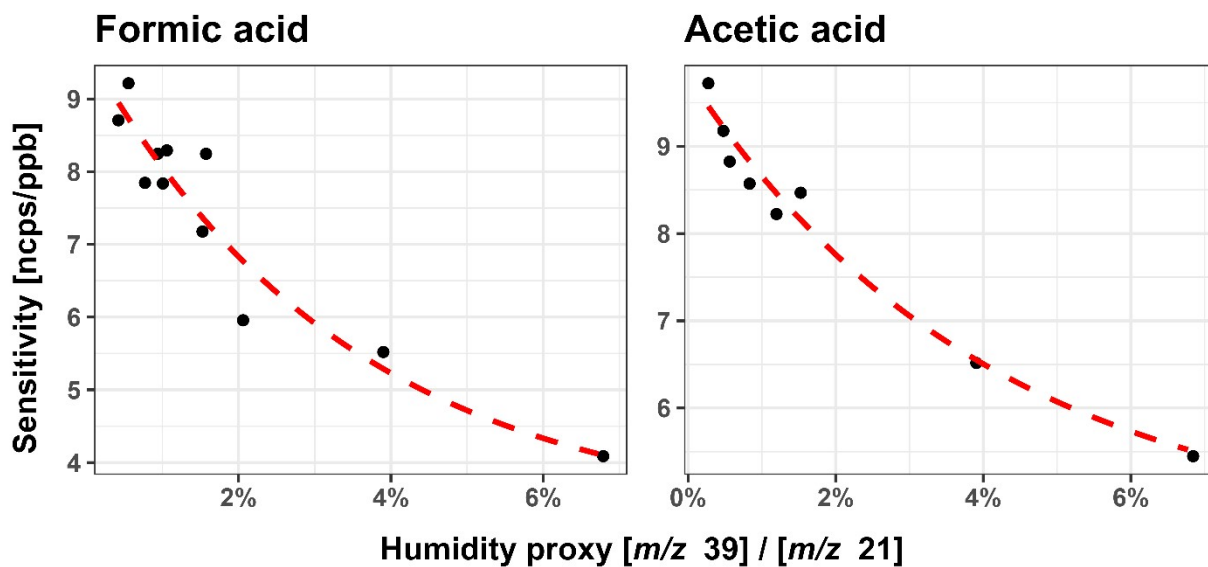


**Figure S2.** Formic and acetic acid sensitivity in PTR-ToF as a function of the internal humidity proxy  $\text{H}_2\text{O}\cdot\text{H}_3\text{O}^+$  to  $\text{H}_3\text{O}^+$  ( $x = [\text{m}/z\ 39]/[\text{m}/z\ 21]$ ). The line of best fit is shown in red, corresponding to:  $y = 6.5e^{-29.1x} + 3.2$  for FA and  $y = 5.3e^{-24.3x} + 4.5$  for AA.

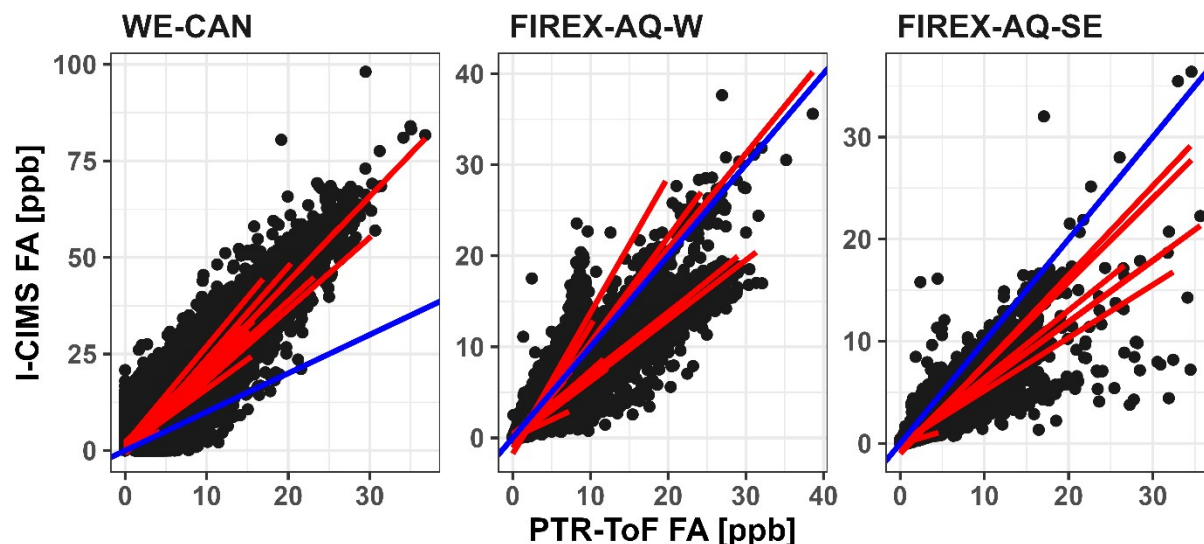


**Figure S3.** Correlations between I- CIMS and PTR-ToF 1 Hz FA measurements for all WE-CAN, FIREX-AQ-W and FIREX-AQ-SE research flights. WE-CAN cloud sampling periods have been removed from the comparison along with FIREX-AQ PTR-ToF FA measurements made above ~4.9 km ASL (< 550 hPa). The blue line represents 1:1 agreement while the red lines are the total least squares regression for each research flight. The equation for the total least squares regression of the aggregated WE-CAN data is  $y = 2.06x + 0.23$  with  $r^2 = 0.82$ ,  $y = 0.89x - 0.26$  with  $r^2 = 0.82$  for FIREX-AQ-W, and  $y = 0.69x - 0.34$  with  $r^2 = 0.67$  for FIREX-AQ-SE.

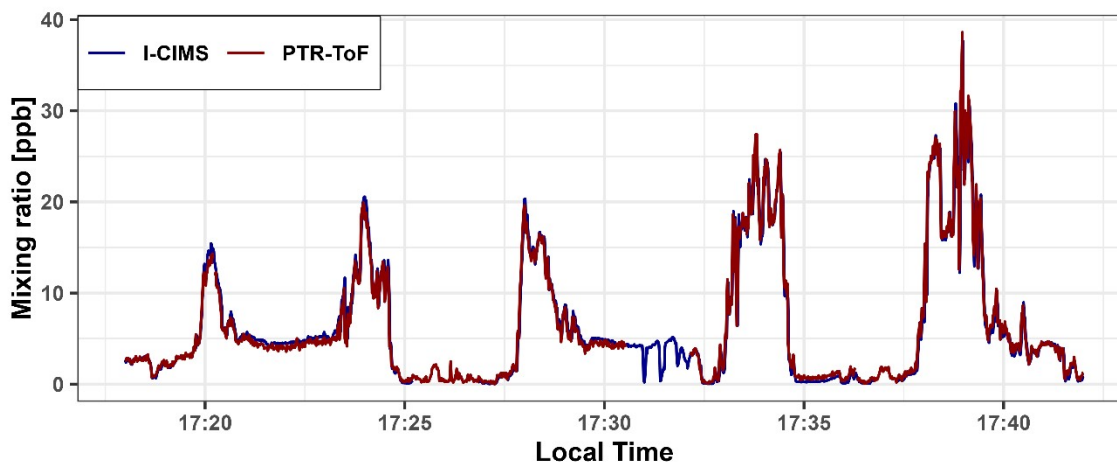


**Figure S4.** Time series of 1 Hz PTR-ToF and I- CIMS formic acid mixing ratios for a subset of pseudo-Lagrangian transects of the Williams Flat Fire, WA, measured during the FIREX-AQ field campaign on August 6<sup>th</sup>, 2019.

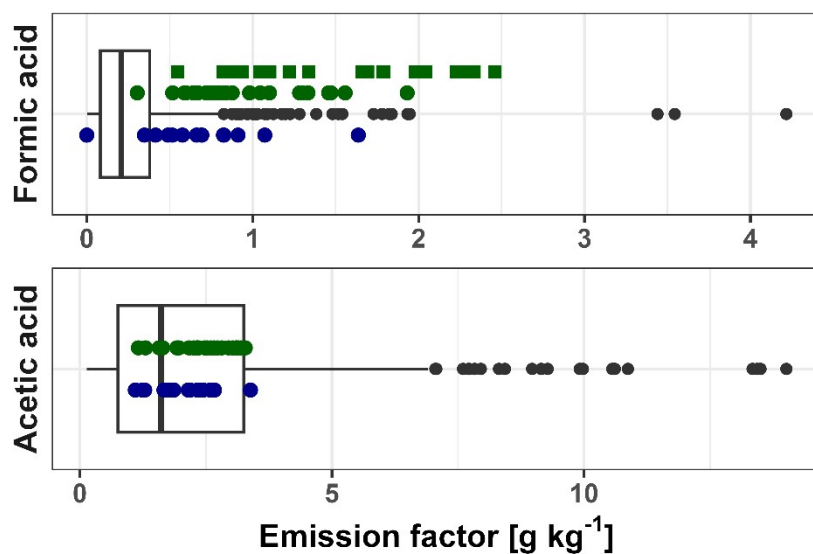


**Figure S5.** Emission factors of formic and acetic acid for literature values (box-and-whisker), WE-CAN PTR-ToF observations (green points), I-CIMS FA (green squares), and FIREX-AQ PTR-ToF (blue points). The box and whisker plots reported include literature EFs from all studies in Table S1 (336 data points for formic acid and 254 for acetic acid). Boxes represent the 25<sup>th</sup> and 75<sup>th</sup> percentiles, vertical lines as median, whiskers as  $1.5 \times$  the interquartile range, and black points as  $> 1.5 \times$  interquartile range.

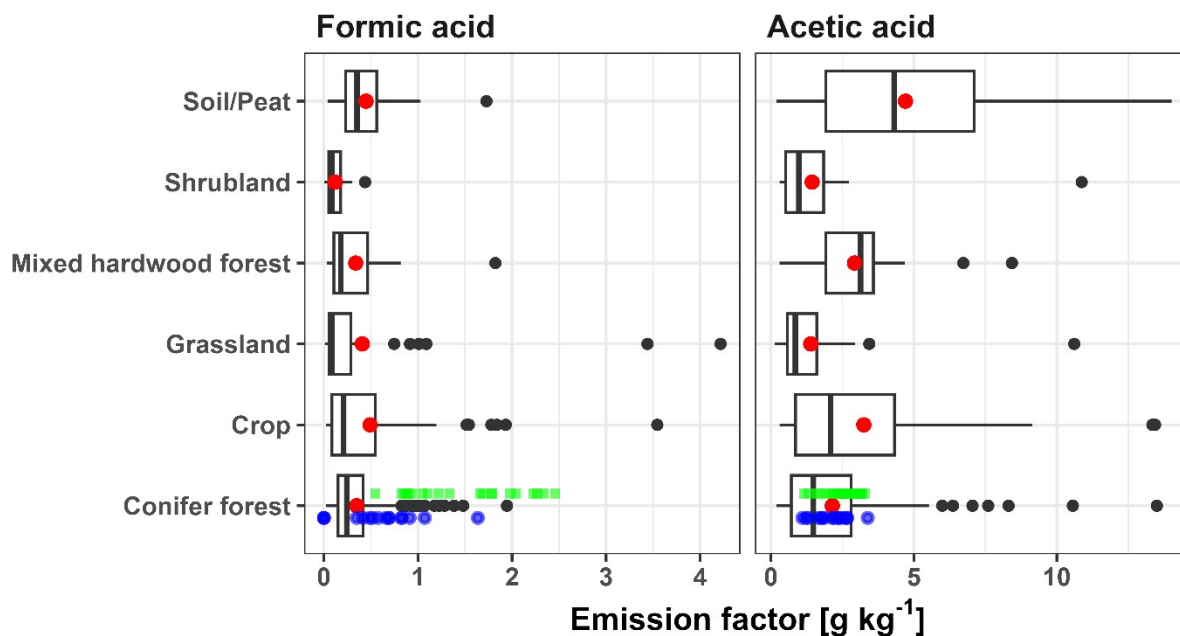


**Figure S6.** Box-and-whisker plot of literature EFs by the type of fuel burned. Red points are the literature mean for the data represented by the boxes, black points are  $> 1.5 \times$  interquartile range of literature values, green squares are WE-CAN EFs measured by I-CIMS, blue points are FIREX-AQ EFs.

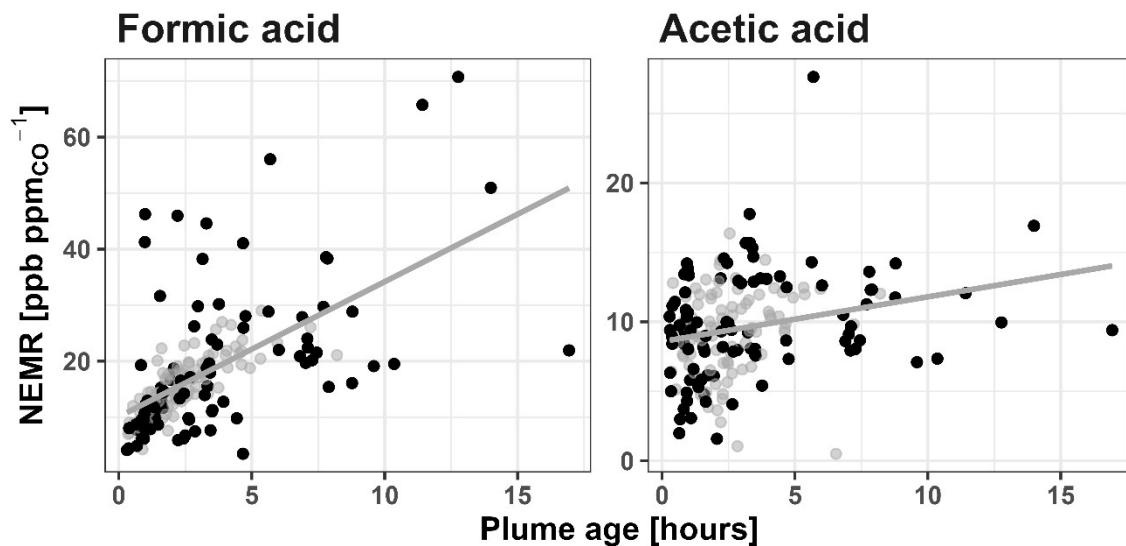


**Figure S7.** NEMRs of FA and AA for all WE-CAN plumes with pseudo-Lagrangian transects. Light gray points are those included in Figure 4, while the black points correspond to the remaining plume transects sampled during the campaign. The least squares regression lines (gray) correspond to all transects and are  $y = 2.4x + 10.1$  ( $r^2 = 0.36$ ) for FA and  $y = 0.32x + 8.6$  ( $r^2 = 0.05$ ) for AA.

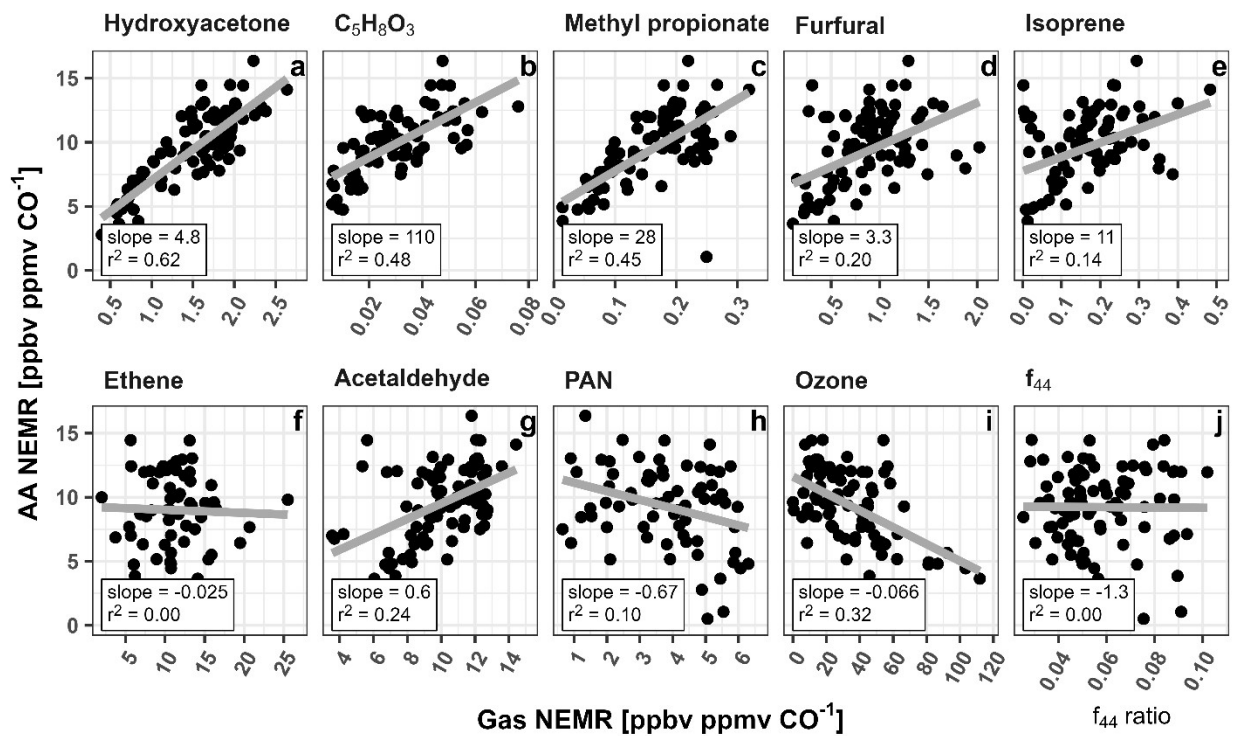


**Figure S8.** AA NEMRs compared to various gas phase species NEMRs and aerosol  $f_{44}$  ratio measured in 5 smoke plumes with more than 10 pseudo-Lagrangian plume transects. Slope and  $r^2$  for the least squares regression of each species are shown at the bottom of each panel, while the gray lines are the best fit. Panels a, b, and c are the three VOCs with the strongest correlation to AA. Panels d and e represent two of the largest OH radical sinks (ranked by OH reactivity from individual VOC)(Permar et al., 2023) that are highly correlated with FA in wildfire emissions. Panels f, and g are known precursors, while h, i and j are representative of the overall plume oxidation. Note, Hydroxyacetone is measured with methyl acetate and Ethyl formate ( $C_3H_6O_2$ ).  $C_5H_8O_3$  = 5-hydroxymethyl tetrahydro 2-furanone. PAN = peroxyacetyl nitrate.  $f_{44}$  = ratio of m/z 44 to the total signal in the aerosol component spectrum with higher ratios indicating more aged organic aerosol and higher O:C.

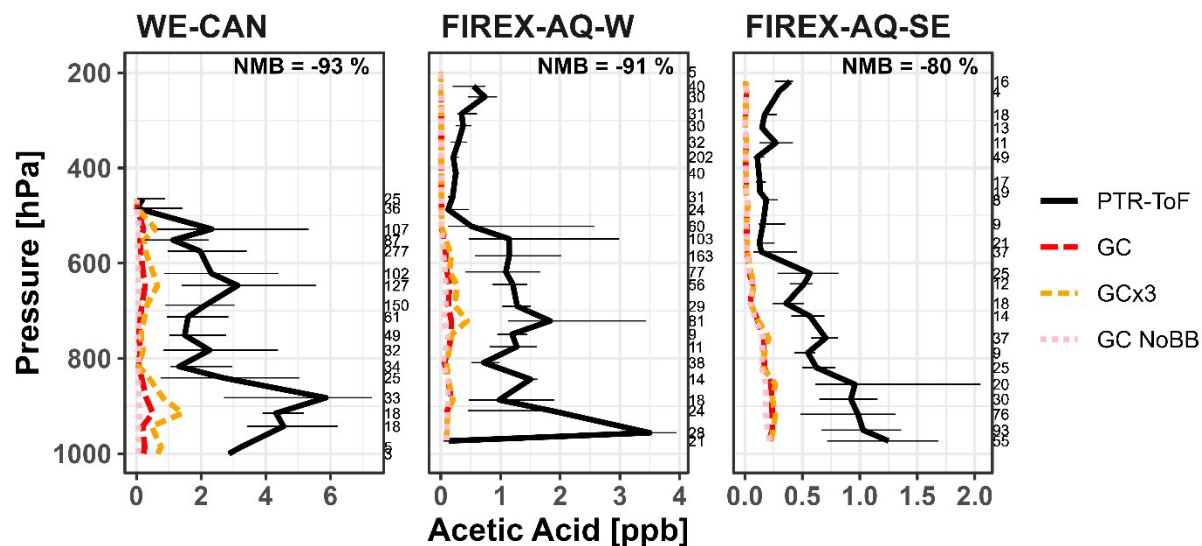


**Figure S9.** Vertical profiles of the median acetic acid mixing ratio measured during the full WE-CAN and FIREX-AQ field campaigns, binned at every 33 hPa. Black lines correspond to the measurements made by PTR-ToF, with error bars representing the 25<sup>th</sup> and 75<sup>th</sup> percentile at each pressure bin. Red dashed lines correspond to GEOS-Chem with GFAS BB emissions (GC), orange dashed lines are GEOS-Chem with 3 × GFAS BB emissions (GC×3), and the pink dotted lines are GEOS-Chem with BB emissions turned off (GC NoBB). The number of samples in each altitude bin are shown on the right of the plots, while the normalized mean bias (NMB) to the I-CIMS measurement for lower altitude observations (> 450 hPa) are shown at the top.

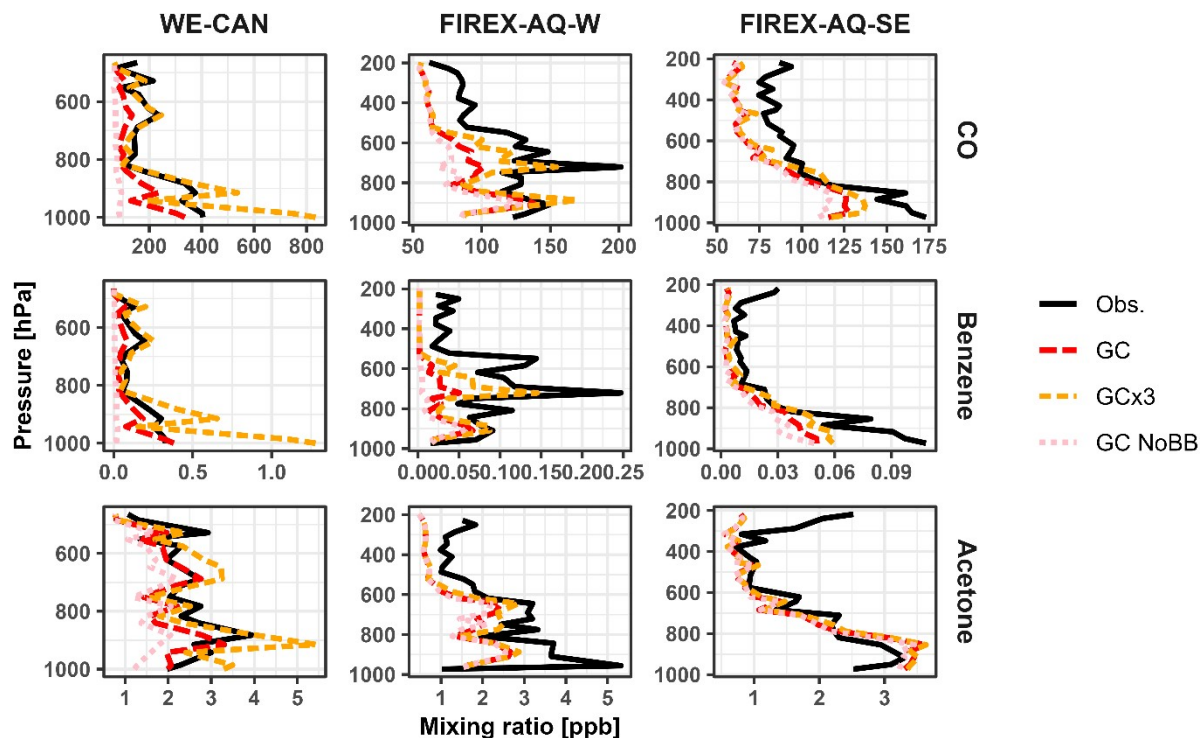


**Figure S10.** Vertical profiles of the median CO, benzene, and acetone mixing ratios measured during the full WE-CAN and FIREX-AQ field campaigns, binned at every 33 hPa. Black lines correspond to the observations while red dashed lines correspond to GEOS-Chem with GFAS BB emissions (GC), orange dashed lines are GEOS-Chem with  $3 \times$  GFAS BB emissions (GC $\times$ 3), and the pink dotted lines are GEOS-Chem with BB emissions turned off (GC NoBB). the pink dotted lines are GEOS-Chem with  $3 \times$  GFAS BB emissions (GC $\times$ 3).

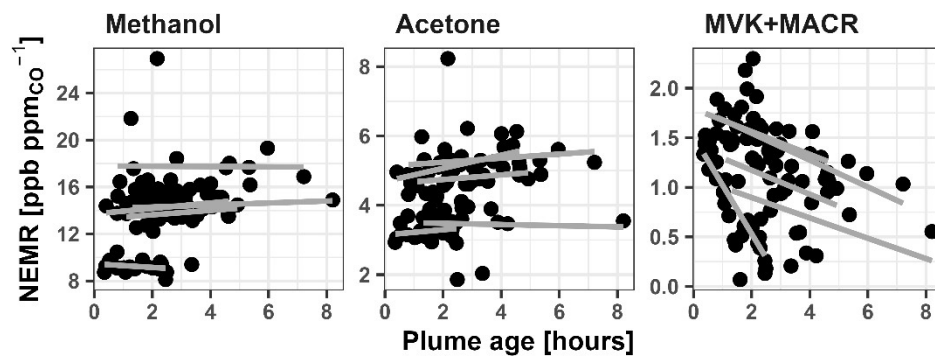


**Figure S11.** NEMRs of methanol, acetone, and MVC+MACR (methyl vinyl ketone and methacrolein) vs. plume age for 5 research flights with more than 10 pseudo-Lagrangian transects during WE-CAN. Least squares regression lines are shown in gray for each fire. Note that acetone is also measured with its isomer propanal.

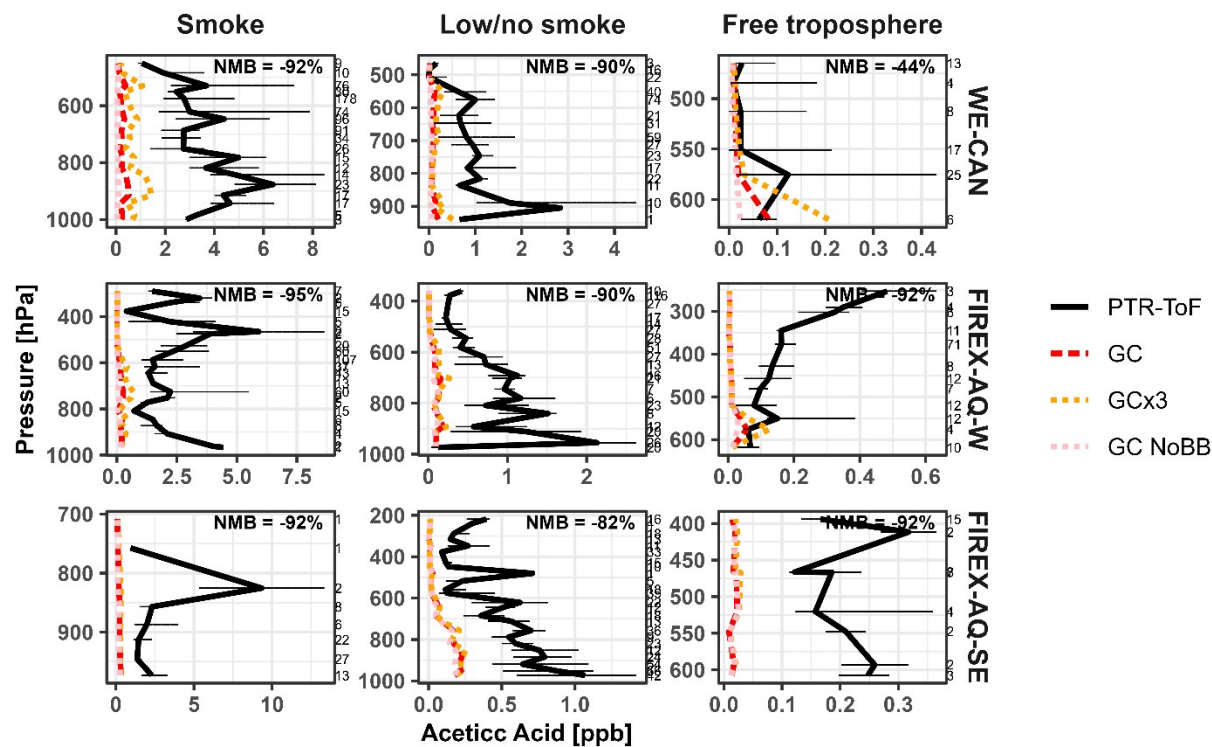


**Figure S12.** Vertical profiles of the median acetic acid mixing ratio measured during the WE-CAN field campaign for smoke impacted, low/no smoke, and free troposphere sampling periods. Pressures are binned at every 33 hPa. Black lines correspond to the measurements made by PTR-ToF. Red dashed lines correspond to GEOS-Chem with GFAS BB emissions (GC), orange dashed lines are GEOS-Chem with  $3 \times$  GFAS BB emissions (GC $\times$ 3), and the pink dotted lines are GEOS-Chem with BB emissions turned off (GC NoBB). Error bars are the 25<sup>th</sup> and 75<sup>th</sup> percentile of the PTR-ToF measurement at each pressure bin.

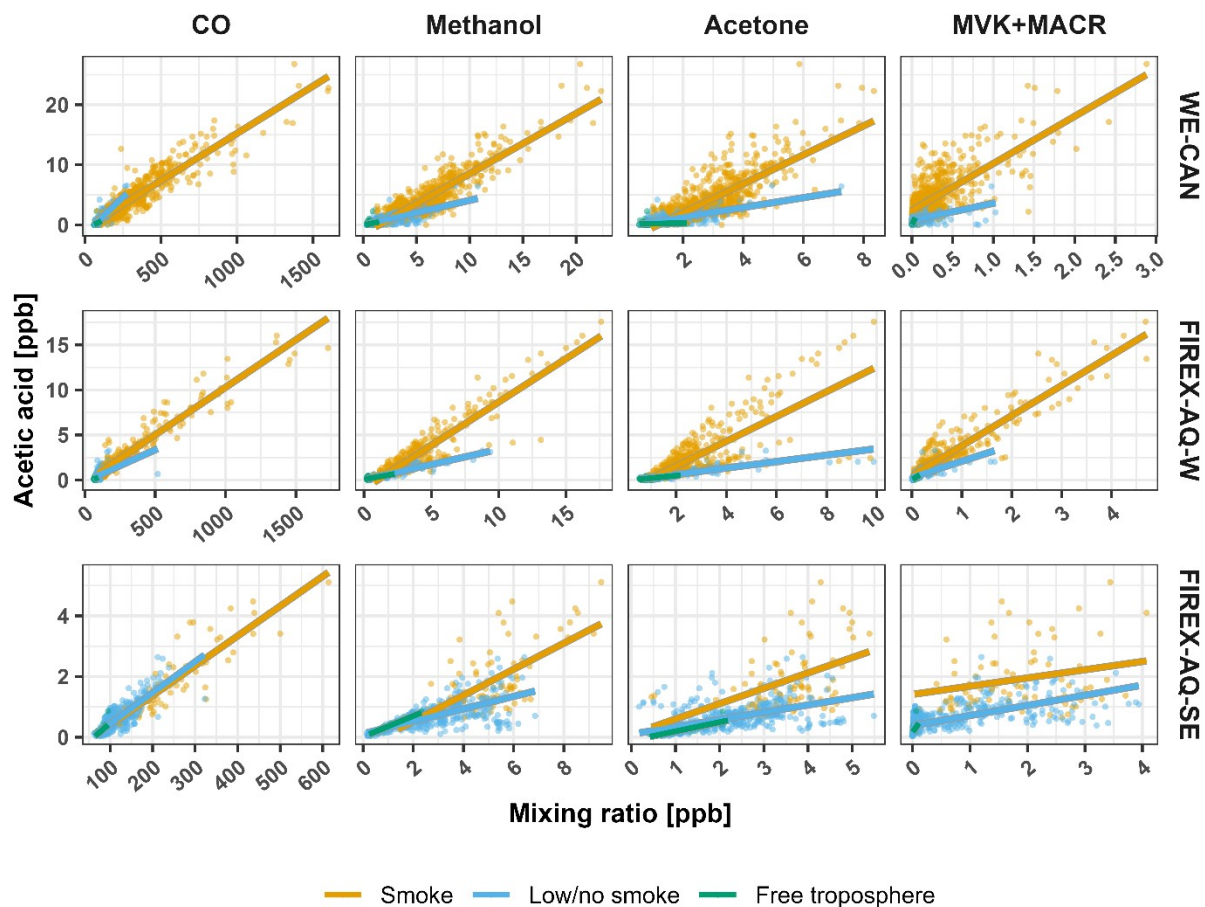


**Figure S13.** Correlations of AA with CO, methanol, acetone, and MVK+MACR (methyl vinyl ketone and methacrolein) during the WE-CAN and FIREX-AQ campaigns. Orange points represent smoke-impacted data, blue points indicate low/no smoke impact, and green points show clean free troposphere measurements (see main texts for definitions). The data have been averaged to 5 minutes. Lines show the least squares regression corresponding to each set of colored points. Note that acetone is also measured with its isomer propanal.

**Table S1:** Average EFs and MCE with  $1\sigma$  standard deviations reported for previous literature, along with the number of observations, if the study came from field or laboratory campaigns, the dominant fuels burned, and instrumentation used. Unreported values are indicated with a “-“, while no standard deviation is shown for single measurements. Instrumentation acronyms include Airborne Fourier Transfer InfraRed (AFTIR) spectrometer, Open-path Fourier Transfer InfraRed (OP-FTIR) spectrometer, Proton Transfer Reaction Mass spectrometer (PTR-MS), and gas chromatograph mass spectrometry (GC-MS).

Study	Formic Acid (g/kg)	Acetic acid (g/kg)	N obs. FA, AA	MCE	Type	Dominant fuel regions	Instrument
Akagi et al., 2013	$0.08 \pm 0.03$	$1.91 \pm 0.95$	5, 10	$0.91 \pm 0.04$	Field	South Carolina USA	AFTIR
Bertschi et al., 2003	$0.59 \pm 0.55$	$4.87 \pm 3.01$	9, 9	$0.87 \pm 0.02$	Laboratory	Montana USA and Zambia Africa	OP-FTIR
Burling et al., 2010	$0.18 \pm 0.23$	$1.57 \pm 2.17$	18, 18	$0.94 \pm 0.03$	Laboratory	Southeast and Southwest USA	OP-FTIR
Burling et al., 2011	$0.09 \pm 0.08$	$1.67 \pm 1.59$	12, 20	$0.91 \pm 0.05$	Field	North Carolina and Southwest USA	AFTIR
Christian et al., 2003	$0.31 \pm 0.28$	$8.35 \pm 4.32$	10, 5	$0.88 \pm 0.05$	Laboratory	Indonesia and Africa	OP-FTIR PTR-MS
Goode et al., 1999	$0.27 \pm 0.22$	$1.28 \pm 0.62$	2, 6	$0.96 \pm 0.01$	Laboratory	Grass fires	OP-FTIR
Goode et al., 2000	$0.54 \pm 0.17$	$2.55 \pm 0.78$	4, 4	$0.92 \pm 0.01$	Field	Alaska USA	AFTIR
Koss et al., 2018	$0.28 \pm 0.22$	-	53	$0.93 \pm 0.04$	Laboratory	Western USA	PTR-ToF-MS
McKenzie et al., 1995	$0.53 \pm 0.4$	$2.64 \pm 2.49$	8, 10	-	Laboratory	Montana USA	GC-MS
Müller et al., 2016	0.13	0.47	1, 1	0.9	Field	Georgia USA	PTR-ToF-MS
Selimovic et al., 2018	$0.28 \pm 0.25$	$1.92 \pm 1.62$	71, 70	$0.93 \pm 0.04$	Laboratory	Western USA	OP-FTIR
Stockwell et al., 2015	$0.28 \pm 0.36$	$2.55 \pm 3.07$	102, 99	$0.94 \pm 0.06$	Laboratory	Mixed global	PTR-ToF-MS
Yokelson et al., 1999	1.48	1.17	1, 1	0.93	Field	North Carolina USA	AFTIR
Yokelson et al., 2003	$0.28 \pm 0.09$	$2.37 \pm 1.05$	6, 6	$0.94 \pm 0.02$	Field	African savanna	AFTIR
Yokelson et al., 2007	$0.28 \pm 0.23$	$3.43 \pm 0.44$	9, 9	$0.91 \pm 0.02$	Field	Tropical and Amazon forests	AFTIR
Yokelson et al., 2011	$1.34 \pm 1.24$	$3.2 \pm 2.52$	19, 21	$0.92 \pm 0.03$	Field	Mexico	AFTIR

**Table S2.** Initialization values used for the Framework for 0-D Atmospheric Modeling of the Taylor Creek Fire.

<b>Compound</b>	<b>Formula</b>	<b>Taylor Creek Fire (ppb)</b>
CO	CO	5670.68
NO	NO	6.76
NO <sub>2</sub>	NO <sub>2</sub>	58.86
HONO	HONO	64.49
Ozone	O <sub>3</sub>	31.75
Furan	C <sub>4</sub> H <sub>4</sub> O	6.33
Benzene	C <sub>6</sub> H <sub>6</sub>	8.10
HNO <sub>3</sub>	HNO <sub>3</sub>	21.00
Guaiacol	C <sub>7</sub> H <sub>8</sub> O <sub>2</sub>	1.05
PAN	C <sub>2</sub> H <sub>3</sub> NO <sub>5</sub>	6.90
Isoprene	C <sub>5</sub> H <sub>8</sub>	1.19
Ethene	C <sub>2</sub> H <sub>4</sub>	82.53
Catechol	C <sub>6</sub> H <sub>6</sub> O <sub>2</sub>	1.00
2-Methylfuran	C <sub>5</sub> H <sub>6</sub> O	1.56
Methylfurfural	C <sub>6</sub> H <sub>6</sub> O <sub>2</sub>	1.00
Dimethylfuran	C <sub>6</sub> H <sub>8</sub> O	0.67
Syringol	C <sub>8</sub> H <sub>10</sub> O <sub>3</sub>	0.07
3-Methylfuran	C <sub>5</sub> H <sub>6</sub> O	0.31
Formaldehyde	CH <sub>2</sub> O	126.05
Acetaldehyde	C <sub>2</sub> H <sub>4</sub> O	53.88
Acetone	C <sub>3</sub> H <sub>6</sub> O	14.34
Propanal	C <sub>3</sub> H <sub>6</sub> O	2.94
MVK	C <sub>4</sub> H <sub>6</sub> O	4.90
MACR	C <sub>4</sub> H <sub>6</sub> O	2.29
PPN	C <sub>3</sub> H <sub>5</sub> NO <sub>5</sub>	0.84
Phenol	C <sub>6</sub> H <sub>6</sub> O	4.23
o-Xylene	C <sub>8</sub> H <sub>10</sub>	0.29
α-Pinene	C <sub>10</sub> H <sub>16</sub>	0.34
p-Xylene	C <sub>8</sub> H <sub>10</sub>	0.75
Cresol	C <sub>7</sub> H <sub>8</sub> O	1.81
1-Butene	C <sub>4</sub> H <sub>8</sub>	5.03
n-Butane	C <sub>4</sub> H <sub>10</sub>	0.90

Ethylbenzene	$C_8H_{10}$	0.59
1,2,3-Trimethylbenzene	$C_9H_{12}$	0.42
Styrene	$C_8H_8$	1.59
Benzaldehyde	$C_7H_6O$	1.07
n-Pentane	$C_5H_{12}$	1.05
n-Hexane	$C_6H_{14}$	0.22
n-Heptane	$C_7H_{16}$	0.18
n-Octane	$C_8H_{18}$	0.11
3-Methyl-1-butene	$C_5H_{10}$	0.27
1-Hexene	$C_6H_{12}$	1.69
$\beta$ -Pinene	$C_{10}H_{16}$	0.22
Acrolein	$C_3H_4O$	5.50
2-Butenal	$C_4H_6O$	1.06
Butanal	$C_4H_8O$	0.27
Pentanal	$C_5H_{10}O$	0.38
Propene	$C_3H_6$	17.43
Butadiene	$C_4H_6$	7.27
Glyoxal	$C_2H_2O_2$	0.29
Sesquiterpenes	$C_{15}H_{24}$	0.02
Methylglyoxal	$C_3H_4O_2$	2.63
Biacetyl	$C_4H_6O_2$	2.43
Formic acid	$CH_2O_2$	51.1
Acetic acid	$C_2H_4O_2$	32.09
Acetol	$C_3H_6O_2$	2.91
Furfural (=furaldehyde)	$C_5H_4O_2$	7.34

---